Experimental Mechanics (2011) 51:879–890
DOI 10.1007/s11340-010-9384-9

Analysis of Cracks and Deformations in a Full Scale Reinforced Concrete Beam Using a Digital Image Correlation Technique

J.-F. Destrebecq · E. Toussaint · E. Ferrier

Received: 20 November 2009 / Accepted: 28 June 2010 / Published online: 28 August 2010

Abstract This paper deals with the use of a digital image correlation technique for the determination of the actual mechanical behaviour of a full scale reinforced concrete beam after 25 years of service in a severe industrial environment. The objective is to investigate the influence of the service conditions on the cracking process and the flexural behaviour of the beam. For this purpose, one beam is removed from the existing structure before being tested in four point bending in laboratory. Displacement fields derived from digital images captured during five loading cycles are analysed in terms of crack detection and measurement, beam deflection and curvature. Owing to its good resolution, the method proves suitable for early crack detection and measurement. A comparison between experimental results and theoretical values derived from Eurocode 2 design code in the serviceability state suggests the existence of a longitudinal compressive force in the beam. A complementary analysis confirms the validity of this hypothesis. It is concluded that the cracking and the flexural behaviour of the tested beam are significantly affected by the existence of an initial compressive stress, which is possibly resulting from a swelling of the concrete due to long term exposure to wet atmosphere and elevated temperature.

Keywords Reinforced concrete · Full scale test · Full-field measurements · Cracks · Deflection · Curvature

J.-F. Destrebecq · E. Toussaint (✉)
Laboratoire de Mécanique et Ingénieries,
Clermont Université, Université Blaise Pascal,
EA 3867, BP 10448, 63000 Clermont-Ferrand, France
e-mail: evelyne.toussaint@ifma.fr

J.-F. Destrebecq · E. Toussaint
CNRS, Fédération de Recherche TIMS FR 2856,
Campus Scientifique des Cézeaux, BP 10125,
63173 Aubière Cedex, France

E. Ferrier
Laboratoire de Génie Civil et Ingénieries
Environnementales Site Bohr, Université Claude Bernard
Lyon I—INSA de Lyon, Domaine scientifique de la DOUA,
82 Boulevard Niels Bohr, 69622 Villeurbanne Cedex, France

Introduction

In situ assessment of actual mechanical state of existing civil engineering structures is an important and difficult task. In the case of reinforced concrete structures, classic measurement techniques such as strain gauges, extensometers, linear variable differential transformer (LVDT) sensors, etc... hardly allow precise estimations of strain fields or early crack detection and local failure processes in deformed structural members. Since the beginning of the eighties, alternative techniques based on full-field measurements have been developed, which allow detailed analyses within a given zone of interest of a loaded structure. One of them is the Digital Image Correlation (DIC) technique [1, 2] which is based on a comparative analysis of digital images of the structural member captured at different deformation states. This technique has been applied successfully to various classes of mechanical and civil engineering structural problems (see [3–5] for instance). Nevertheless, at the authors' knowledge, the number of experimental studies combining civil engineering structures and DIC technique is limited. They concern small structures (see [6, 7] for instance) or

larger ones (see [8–10] for instance), although most of them concern models of civil engineering structures or parts of them. Very few experiments have been performed on full scale structures, in laboratory or *in situ* (see [11]). Besides, the published matter is generally limited to the use of displacements fields for crack detection and measurements.

The present study is dedicated to a full scale reinforced concrete beam previously in use in an industrial environment over a 25 years period. The beam was a part of a huge concrete structure subjected to sustained loading, and exposed to wet atmosphere and elevated temperature during its service lifespan. Some damages were observed in the structure, involving a need for an estimation of the actual mechanical state of the structure components. To this aim, several beams were removed from the structure, and they were transported to laboratory for full scale testing. The beam concerned in this study was devoted to the determination of the actual flexural behaviour and the cracking process by means of a digital image correlation technique.

The first part of this study is dedicated to the presentation of the experimental program. For this purpose, the tested beam, the DIC technique used and the experimental set-up for testing the beam in cyclic four points bending are presented. In the next section, the DIC technique is applied to crack detection and to crack width measurements, based on the analysis of displacement fields during five loading cycles. Obtained distances between neighbour cracks are compared with visual measurements performed on the beam during the test. Then, the displacement fields given by the DIC technique are analysed in order to determine the evolution of the beam deflection and the flexural curvature during the loading cycles. It is shown that, owing to the good resolution of the method, the DIC technique is suitable for early crack detection and crack width measurements. Finally, the last section of the study is devoted to a theoretical analysis of the crack widths and the curvature in terms of the applied loading. Based on a comparison between experimental results given by the DIC technique and theoretical values derived from Eurocode 2 design code provisions in the serviceability state [12], it is shown that the flexural behaviour and the cracking process are significantly influenced by the existence of initial compressive stresses in the beam cross-section. This initial stress state possibly resulted from a swelling process of the concrete exposed to wet and warm atmosphere during the 25 years of service.

Experimental Setup

Description of the Tested Beam

The reinforced concrete beam concerned in the present study was a part of a huge concrete structure subjected to sustained loading. It was exposed to saturated water steam at an approximately steady temperature about 35°C during 25 years of service life. The beam was statically determinate in the structure. It was removed from the structure and transported to laboratory for full scale testing. A residual deflection, about 2.6 mm, could be observed after unloading, possibly due to irrecoverable creep. The external surface of the beam was covered with a thin layer of tartar due to the exposure of the structure. No evidence of damage could be seen, excepted at both ends which were damaged when the beam was removed from the structure. There were no visible cracks on the surface of the beam, but the existence of closed cracks under the tartar layer could not been excluded. The aim of the present study is to investigate various aspects of the actual mechanical behaviour of the beam (i.e. cracking, curvature and deflection) by means of a full field measurement method.

The main dimensional characteristics of the beam are as follows: 7,840 mm in length, with a $160 \times 450\ \text{mm}^2$ rectangular cross-section (see Fig. 1). The longitudinal reinforcement consists of four deformed steel bars, 14 mm in diameter. The transversal reinforcement consists of vertical stirrups, 6 mm in diameter with a constant spacing equal to 170 mm (the spacing is reduced at both extremities of the beam). Preliminary compression tests were performed on concrete core cylinders drilled out from a companion beam. Since the beams were precast, it is assumed that both beams exhibit similar material properties. The actual mechanical

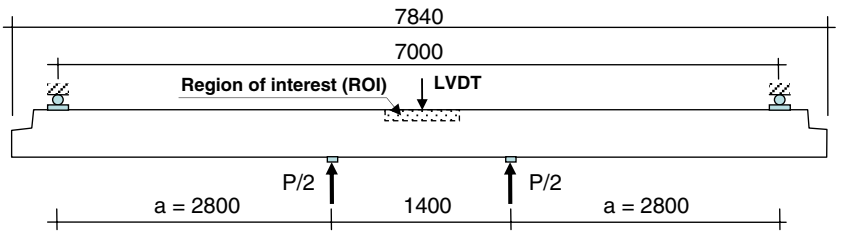

Fig. 1 Lay-out of the beam tested in four point bending (lengths in mm)

characteristics of the concrete were found as follows, based on NF EN12 390-4 standard compression tests: ultimate compressive strength equal to 29.8 MPa ± 1.7 MPa , and actual longitudinal Young modulus equal to 30.1 GPa ± 0.8 GPa. No evidence of corrosion could be observed at the surface of the reinforcing bars.

The Digital Image Correlation Technique

The full field measurement method used in the present study is based on the Digital Image Correlation (DIC) technique. It was first proposed by Sutton [1]. This technique is based on a comparison between two digital images of the sample surface captured at two different levels of loading. It requires a random distribution of the grey levels on both pictures. This can be easily achieved by spraying small black or white paint spots on the sample surface in order to create a contrasted random pattern. A Region of Interest, denoted as ROI, is chosen in the reference image. In the present study, it corresponds to a rectangle-shaped area, 718 × 102 mm in size, located between the two loading points in the tension zone of the beam (see Fig. 1). A close view of the ROI is shown in Fig. 2(a). The ROI extends downward from the top surface of the beam. Its depth is limited by the existence of a lighting device (wide horizontal black strip on the picture) positioned between the camera and the beam, aiming at ensuring uniform lighting condition of the beam lateral face.

The ROI is divided into a number of square-shaped grid elements. Each element is called a Zone of Interest (ZOI). Centered on each of the four corners of a ZOI, a square-shaped zone called the correlation pattern is used for the DIC analysis of the images. The dashed line in Fig. 2(a) indicates the horizontal location used for crack detection and measurement in Section "Crack Measurements".

The analysis consists in matching the former image (called reference image) and the second one (deformed image) in relation to their grey level distributions. For this purpose, the initial grey level distribution in the reference image is represented by a function $f(x, y)$. This function becomes $f^\star(x^\star, y^\star) = f^\star((x + u(x, y), y + v(x, y))$ in the deformed image, where $u(x, y)$ and $v(x, y)$ are the components of the displacement field onto the surface under investigation. A correlation coefficient is calculated for each correlation pattern, which is based on the grey level distributions in the reference and the deformed images. It is worth noticing that the correlation coefficient is independent of a modification of the relative average grey level between the two images. An iterative process based on an optimization of the correlation coefficient calculates the relative displacement components (i.e. $u(x, y)$ and $v(x, y)$) between the two images at the nodes of every ZOI within the ROI attached to the investigated surface. This procedure provides discrete values of the displacement components. A continuous displacement field can be obtained by interpolation between the node values.

A 2D image correlation system is used in the present study.

The images are shot with a 12 bits dynamic Philips camera connected to a personal computer. The CCD camera has 10^6 joined pixels (1,024 × 1,024 pixels^2). The images are processed using a DIC software called SeptD and developed by Vacher [13]. The quality of the measurement can be quantified by two quantities.

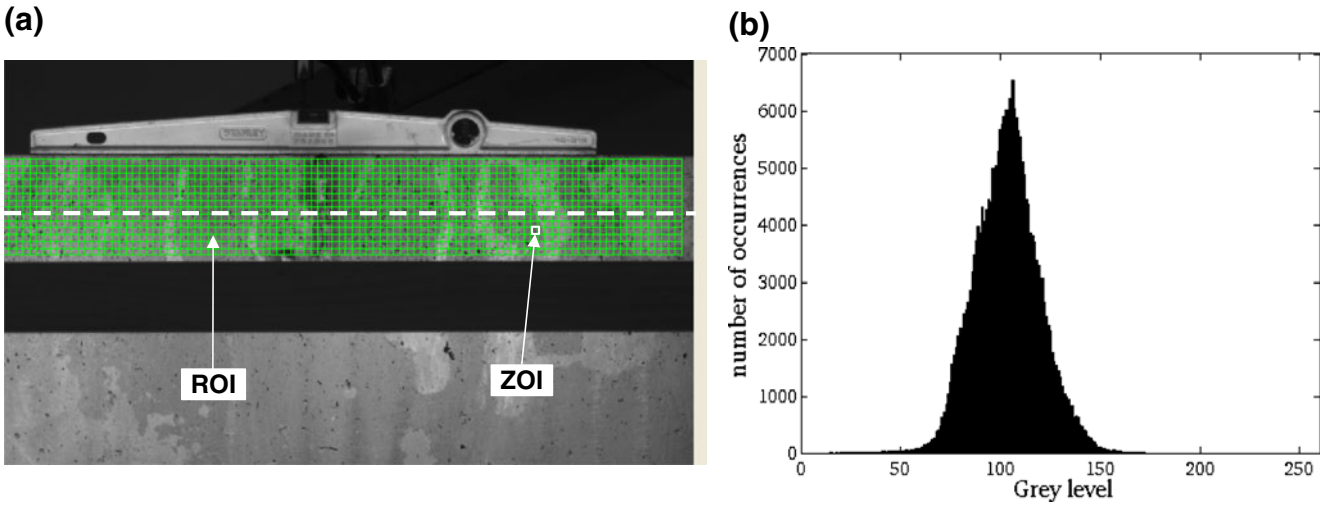

Fig. 2 Close view of the ROI on the beam lateral face (**a**) and corresponding histogram of grey levels (**b**)

The one is the spatial resolution, which is the smallest distance between two independent points. This distance depends on the quality of the random pattern on the sample surface; it must be considered while choosing the size of the ZOI. The other is the resolution, which is the smallest detectable measurement. It depends on the quality of the equipment (camera, lighting), and it can be defined as the standard deviation of the noise.

Description of the Test

The beam was tested in four-points bending the upside down as shown in Fig. 1. Since the extremities of the beam damaged when they were disconnected from the structure, it was decided to reduce the distance between the supports to 7,000 mm for the test (instead of 7,680 mm *in situ*). The loading was applied by means of two hydraulic jacks located at a distance of 700 mm both sides of the mid-span of the beam. By this way, it was possible to apply a preloading in order to counterbalance the dead weight of the beam, then to increase the loading forces in order to get a complete description of the beam behaviour starting from a zeroed bending moment in the mid-span cross-section.

Rather limited efforts were needed to prepare the beam in order to use the DIC technique. A LVDT sensor was positioned at mid-span in order to measure the beam deflection in the course of test. A region of interest was defined in the tensile zone on the lateral surface of the beam, between the two loading points (ROI in Fig. 1). The size of the ZOI was chosen equal to 10×10 pixels^2, leading to a spatial resolution equal to 10 pixels. Owing to the light grey colour of the concrete surface, only black paint spots were sprayed onto the ROI to create a random contrasted pattern. The quality of the random grey level was analysed in term of histogram. Figure 2(b) presents the histogram of grey level within the ROI on the concrete specimen surface.

It is worth noticing that the SeptD sofware used for DIC processing treats 8 bit images only, leading therefore to 256 grey level scaling.

A Gaussian shaped distribution indicates that the random pattern is satisfactory and that the image correlation technique can be successfully processed.

The smallest detectable measurement is the resolution; it can be defined as the standard deviation of the noise. It depends on the quality of the contrasted random pattern, i.e. the spot sizes, the spot number by area unit, the randomness of the pattern and the contrast in terms of grey level. In the present study, the resolution was found to be equal to about 0.01 pixels. For that purpose, two images were captured before loading; they were compared using SeptD software and the standard deviation of the noise was calculated. Owing to the size of the ROI, the focus of the camera was adjusted so that one pixel on the picture corresponded to 0.725 mm on the beam. For a ZOI of 10×10 pixels with a pattern of 10×10 pixels (meaning that the distance between two independent points was equal to 10 pixels), the mean standard deviation for the transversal and longitudinal fields was found equal to 0.0097 pixels (ie. 7.05 μm).

The testing program consisted of five loading cycles. Four loading-unloading cycles were first applied with a maximum value of the loading force equal to 50 kN. This value is in accordance with the maximum loading condition of the beam observed during its *in situ* service life. A minimum value equal to 5 kN upon unloading was assigned to the loading force. During the fifth loading cycle, the loading force was increased until the bending failure of the beam occurred. Based on usual methods suitable for RC-beams design [12], the ultimate value of the loading force at failure was estimated about 80.9 kN in the test conditions.

Vertical displacements measured by the LVDT sensors were continuously recorded during the five loading cycles. Simutaneously, digital pictures of the ROI were captured by means of the digital camera and stored in a computer at various loading stages during the test. One picture was captured before loading; it was used as a reference image for the DIC processing. Additional pictures were captured at every 5 kN during the ascending branch of each loading cycle. The pictures were post-processed in order to determine the horizontal and vertical components of the displacement field throughout the region of interest for every loading level.

From the analysis of the displacement field, it is expected to detect the cracks formation in the tensile zone of the beam, and to determine the evolution of the cracks opening in relation with the loading level. It is also expected to determine the evolution of the deflection and the curvature in the bent beam during the test.

Full-field based DIC methods have been proposed for strain determination in a homogeneous steel girder [14], or for crack measurement in a silicon carbide sandwiched beam [15]. In the case of a cracked reinforced concrete beam, the displacement field is complex due to intricate interaction mechanisms between concrete, cracks and embedded steel bars. The present study aims at analyzing the progressive cracking process and the actual flexural behaviour of the beam by means of a DIC technique in comparison with usual design provisions [12]. Therefore, the methodology is adapted to this aim: the cracks are analyzed from longitudinal displacement measurements in the vicinity of the

steel reinforcement, and the flexural behaviour is determined from vertical displacement measurements at mid-distance between neighbour cracks in order to minimize possible perturbations due to the cracks.

Crack Measurements

The distribution of the longitudinal displacement in the tensile zone of a reinforced concrete beam is strongly affected by the cracking process. The longitudinal component of the displacement field can be measured with a good resolution by means of the DIC technique as soon as the loading is being applied. Therefore, this technique gives an opportunity for easy crack detection and measurements.

In this section, the Digital Image Correlation technique is used to investigate the cracking process and the opening of cracks during the test. The images captured at different levels of loading are processed in comparison with the reference image captured before loading. The processing gives the displacement field in the ROI during the test. In a first stage, the results of the DIC analysis are used for detecting the crack formation and determining their locations in the tension zone of the beam. In a second stage, they are used to analyse the crack openings during the loading cycles. Owing to the brittleness of the thin tartar layer, it is assumed that it has no significant influence on the crack measurements.

Crack Detection

Figure 3 shows an example of the longitudinal component distribution of the displacement field given by the DIC technique for six different levels of loading at a distance of 59 mm from the tensile soffit of the beam, i.e. at mid-distance between the two tensed reinforcing bars.

Similar curves are obtained by averaging longitudinal displacement values obtained along three, five or seven ZOI lines. Therefore, the analysis is based on the displacement values given by one ZOI line only.

The following method is applied for the analysis of this figure, in order to determine the location and the opening of every crack within the ROI:

- every discontinuity in the longitudinal displacement component reveals the existence of a crack,
- the abscissa at which the discontinuity occurs gives the location of the crack (same for the all loading levels),

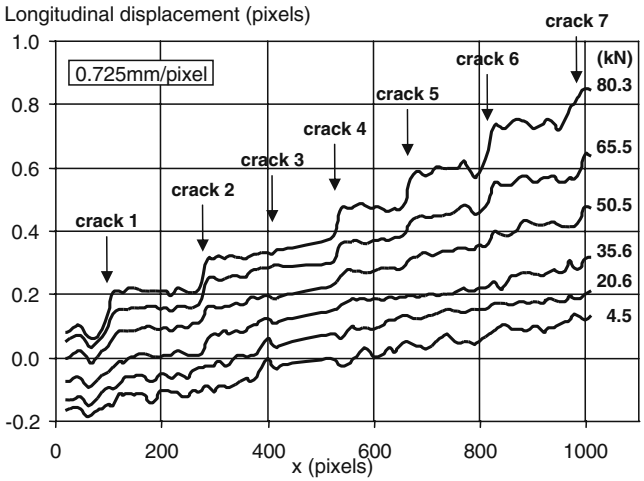

Fig. 3 Crack detection and measurement from the longitudinal displacement component at mid-distance between the tensile steel bars for six different levels of loading (for the sake of clarity, each curve is shifted vertically by 0.1 mm in order to have it separate from the others)—cycle 5

- the vertical amplitude of the discontinuity corresponds to the crack opening (increasing with the loading level).

Looking at Fig. 3, seven cracks are detected within the ROI in the tensile zone of the tested beam. The distances between neighbour cracks are obtained by difference between the relevant crack locations. A visual detection of the cracks was performed at the end of the test, just before bending failure, in order to verify the information given by the DIC technique. The measured values are compared with the observed ones in Table 1. It is obvious that the two sets of values are in fair agreement. The small differences between the measured and the observed values can be due to the fact that the visual crack detection was performed at the uppermost tensile soffit of the beam. It is worth noticing that visual crack detection requires a very close inspection of the concrete surface in the tensile zone of the beam. To make sure that all cracks will be detected, the loading must be given a sufficient level. On the contrary, the DIC technique only requires digital images of the cracked concrete surface: looking at the set of curves in Fig. 3, the progressive formation of cracks at low loading levels is confirmed by the obvious discontinuities in the longitudinal displacement component at higher loading levels. Therefore, owing to the high resolution of the method, and taking advantage of the possibility to compare images captured at different levels of loading, this technique is suitable for early detection and precise location of cracks for low cost preparation work.

Table 1 Crack locations and spacings

Crack number	1	2	3	4	5	6	7	Average
Location (mm) / visual	−260	−125	−60	+71	+150	+261	+390	
Location (mm) / DIC	−258	−126	−64	+52	+150	+259	+389	
Spacing (mm) / visual	135	65	131	79	111	129		108.3
Spacing (mm) / DIC	132	62	116	98	109	130		107.8

Crack Widths

As it was already stated in Section "Crack Detection", the actual crack widths in the loaded beam are reflected by the amplitude of the vertical steps in the plotted longitudinal component of the displacement (see Fig. 3). This statement is used to determine the evolutions of the crack widths during the test. This is achieved by processing the pictures captured at every 5 kN during the five loading cycles. Figures 4 and 5 show the evolutions of the seven crack widths vs. the loading force during the ascending branch of cycles 1 and 5, respectively. Crack widths obtained for cycles 2–4 are very similar to Fig. 4. It is obvious that all cracks don't behave in the same way. Large widths are observed for cracks 1 and 2. Smaller widths are observed for the other cracks which behave more or less in a similar manner. Crack 3 proves almost inactive; its width hardly overcomes 0.02 mm during the whole test.

As it exists, it contributes anyway to the cracking and the flexural behaviour of the tested beam. Therefore, it is taken into account in the following.

The crack width distribution can be analysed in terms of mean value and standard-deviation calculated for the seven cracks at each loading level. The results are shown in Fig. 6. Each of solid lines represents the mean width evolution during a given loading cycle. It is obvious that the mean crack evolutions are very similar for the five loading cycles. The dashed lines represent the 10% lower limit and the 90% upper limit of the width measurements for the five loading cycles. Such a scatter is not unusual; indeed, it is inherent to the cracking process in reinforced concrete members.

However, a difference is observed in Fig. 6 between cycle 1 and the others for low loading levels. The existence of initial widths greater than zero for cycles 2–5 reveals that most of the cracks do not completely close upon unloading. This can be due to interlocking effects which prevent cracks from closing. Figure 5 shows that not all cracks are affected to the same extent by this phenomenon.

Finally, the DIC technique used in this study proves suitable for precise assessment of the cracking process in the tensile zone of the beam. The results presented above are consistent with the expected resolution (see Section "Description of the Test"). One of main advantages of the technique is that previous visual detection of cracks is not necessary for width measurements. It is therefore suitable for early measurements of crack widths, starting from an uncracked state.

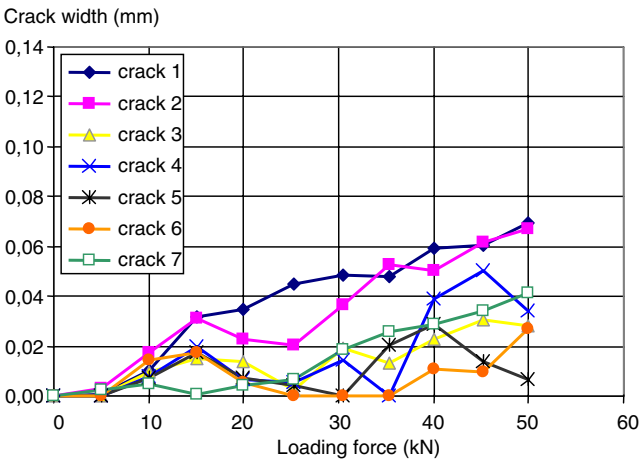

Fig. 4 Crack widths versus loading force during cycle 1

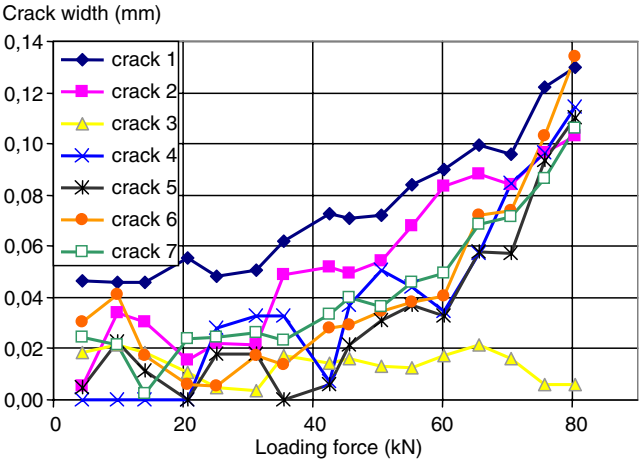

Fig. 5 Crack widths versus loading force during cycle 5

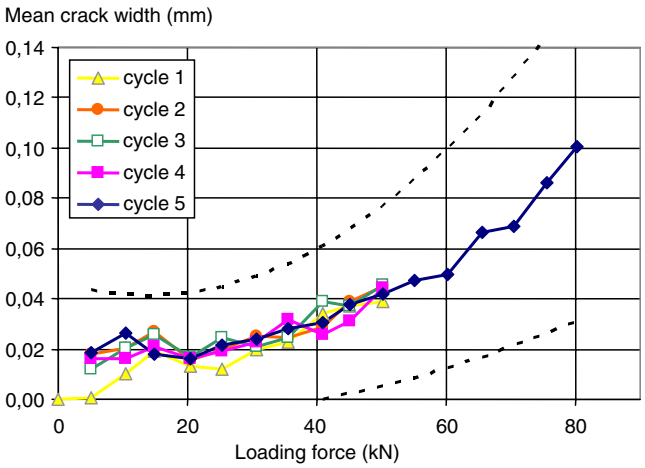

Fig. 6 Mean crack widths versus loading force—cycles 1–5

Deflection and Curvature Measurements

Principle of the Method

From the knowledge of the displacement field it is possible to derive the evolutions of the deflection and the flexural curvature in the beam during the loading cycles. In order to minimize the influence of the cracking on the concrete strain state, it is decided to base the analysis on local values of the vertical displacement component given by the DIC technique at mid-distance between every couple of neighbour cracks. The method is divided in three steps as follows:

- Local values of the deflection at a given load are estimated by averaging the vertical displacement component given by the DIC technique along six vertical lines located at mid-distance between every couple of neighbour cracks. As seven cracks are located in the ROI, six local values of the deflection are obtained.
- The values obtained are plotted against the horizontal position along the beam. Having in mind that the beam is tested in four-point bending, the six points are fitted by a second degree polynomial in order to represent the averaged deflection line along the beam.
- The maximum beam deflection corresponds to the value of the polynomial curve at mid-span. The averaged curvature is equal to twice the coefficient value of the highest degree of the fitted polynomial.

The method is applied to each processed image (i.e. at every 5 kN) during the five loading cycles.

Deflection Measurement

An example of the displacement vertical component given by the DIC technique is shown in Fig. 7, where the vertical displacement along the vertical line located at mid-distance between cracks 1 and 2 is plotted for a load of 40.9 kN (cycle 2). The average value obtained for the local deflection is equal to 8.542 mm with a standard deviation of 0.024 mm, which corresponds to a variation coefficient about 0.28%. This representative example shows the good resolution of the DIC technique for deflection determination.

The same procedure is repeated for the six vertical lines located between the cracks, for every intermediate step of loading during the five loading cycles. As an example, the averaged vertical displacements obtained for the six vertical lines vs. the horizontal position are plotted in Fig. 8 for the five cycles at the same loading level equal to 40.9 kN. The fitted deflection lines obtained for cycles 2–5 prove very similar. The one obtained for cycle 1 is slightly lower than the others.

The beam deflection corresponds to the vertical displacement at mid-span. It is easily derived from the expression of the fitted deflection line for each intermediate level of loading during the test. Figure 9 presents the deflection plotted against the load for the whole test. In this figure, the values given by the LVDT sensor (solid line) are compared with the values obtained with the DIC technique (marks) during the ascending branches of the five loading cycles. It is observed that cycles 2–5 are pretty similar, and that the discrepancy between DIC and LVDT values is negligible for all

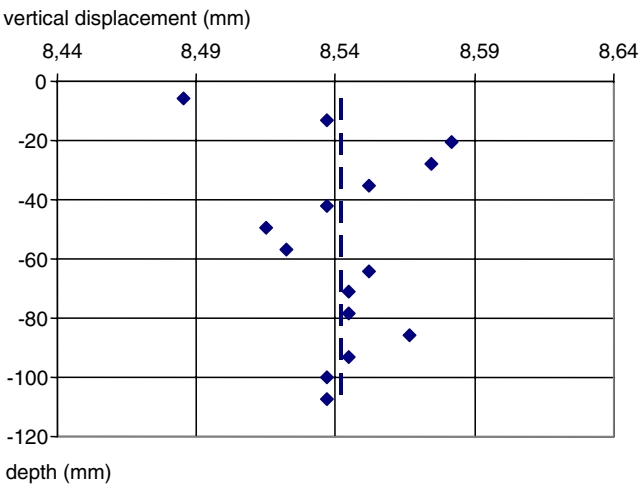

Fig. 7 Vertical displacement at mid-distance between cracks 1 and 2—cycle 2 (40.9 kN)

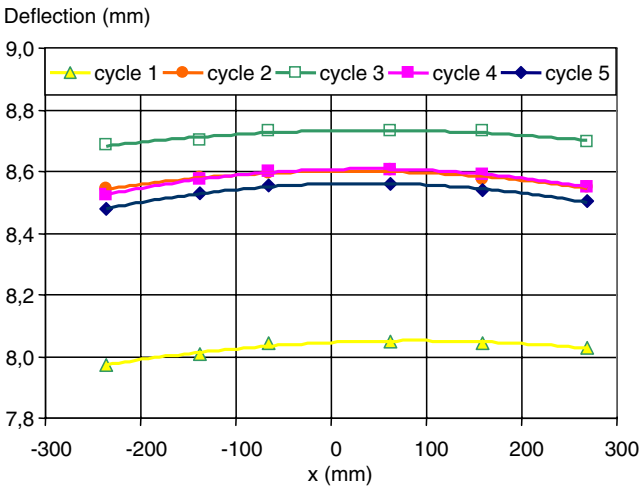

Fig. 8 Vertical displacement vs horizontal position: measured from DIC technique (*marks*), fitted second degree polynomial (*solid lines*)—cycles 1–5 (40.9 kN)

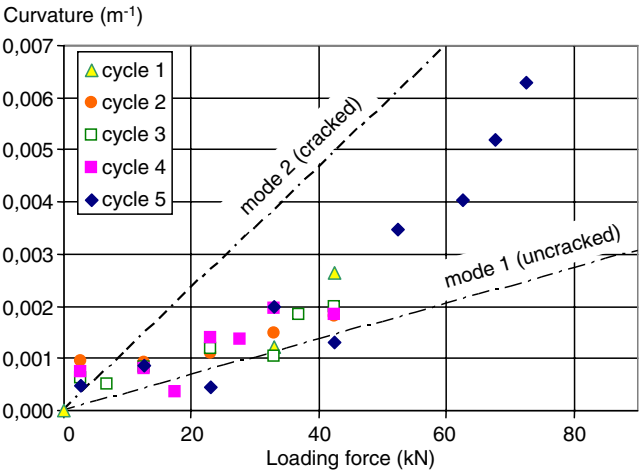

Fig. 10 Curvature vs load, theoretical (*interrupted lines*) and experimental using DIC technique (*marks*)—cycles 1–5

cycles up to 50 kN. A difference is however observed over this limit during cycle 5. It is concluded that the DIC technique used in this study is suitable for fair deflection measurement on full scale structural members.

Curvature Measurement

The flexural curvature at a given load is derived from the fitted deflection line shown in Fig. 8. As it was stated before, the curvature corresponds to twice the coefficient value of the highest degree of the interpolation polynomial. Figure 10 presents the evolution of the curvature plotted against the load during the five loading cycles.

For the sake of comparison, two lines corresponding to the theoretical behaviour of the reinforced cross-section in an uncracked state (mode 1) and in a cracked state (mode 2) [12] are plotted on the same figure. It is observed that the evolution of the flexural curvature of the beam can be analyzed in two stages: although cracks have already formed in the tensile zone of the beam (see Section "Crack Widths"), the beam behaves as in uncracked mode 1 up to about 30 kN; over this limit, the beam flexural behaviour turns parallel to cracked mode 2. This behaviour suggests the existence of an initial compressive stress state in the beam before application of the external loading. The next section will be devoted to an analysis of the test results based on this hypothesis. The existence of a residual curvature is observed for low values of the loading force. This can be caused by the incomplete closing of the cracks at unloading, as already mentioned in Section "Crack Widths."

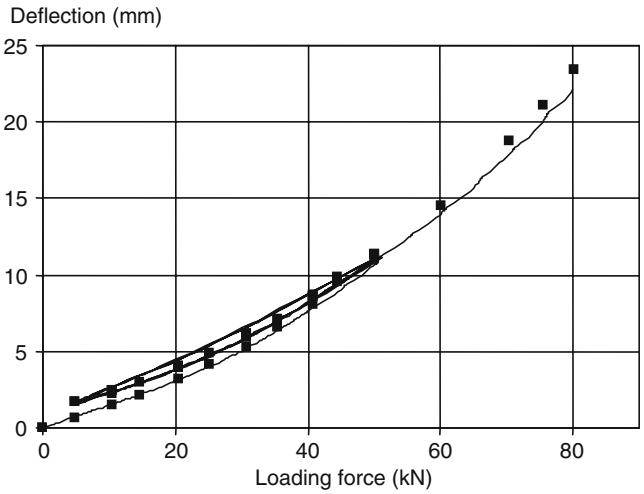

Fig. 9 Mid-span deflection vs load from LVDT measurement (*solid line*) and from DIC technique (*marks*)—cycles 1–5

Analysis and Discussion

Analysis of a Cracked Cross-section

Based on usual assumptions for the analysis of a reinforced concrete beam in the serviceability state [12], the kinematics equations for a cracked cross-section subjected to a decentred longitudinal force N (see Fig. 11) reduces to the following governing equation

$$S - \frac{I}{e} = 0 \Rightarrow e = \frac{I}{S} \tag{1}$$

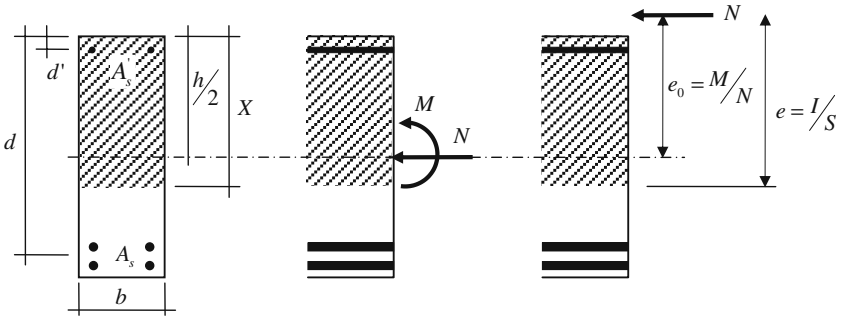

Fig. 11 Cracked cross-section subjected to a decentred longitudinal force (*dashed areas* represent compressed concrete zones)

where e is the eccentricity of the longitudinal force measured from the neutral axis in the cracked cross-section. S and I denote the first and the second moment of inertia of the transformed cracked cross-section respectively; they are written as follows in terms of the depth X of the compressive zone in the cross-section

$$S = \frac{b\,X^2}{2} + \alpha A_s' \left(X - d'\right) + \alpha A_s (X - d) \tag{2}$$

$$I = \frac{b\,X^3}{3} + \alpha A_s' \left(X - d'\right)^2 + \alpha A_s (X - d)^2 \tag{3}$$

In the above equations b is the width of the beam cross-section, and α is the steel to concrete Young's modulus ratio. A_s' and A_s are the cross-sectional areas of the Re-bars located in the compressive and the tensile zone of the beam respectively, at distances d' and d from the compressed face of the cross-section.

The curvature χ caused by the decentred longitudinal force N in the cracked cross-section is written as:

$$\chi = \frac{Ne}{E_c I} \tag{4}$$

where E_c denotes the Young's modulus of the concrete. The tensile steel stress corresponding to this curvature is:

$$\sigma_s = E_s \chi (d - X) = \alpha \frac{Ne(d - X)}{I} \tag{5}$$

where E_s denotes the Young's modulus in the steel bars (assumed as 200 GPa in the present work).

Finally, having in mind that $e_0 = e - X + h/2$ and $e_0 = M/N = Pa/2N$, where h is the beam depth (see Fig. 11), and a is the distance between one support and the nearest jack (see Fig. 1), the following relationship between the loading force P, the longitudinal force N and the compressive zone depth X is obtained

$$P = \frac{N}{a}\left[2\left(\frac{I}{S} - X\right) + h\right] \tag{6}$$

According to [12], the average crack width w_m caused by a short term loading is:

$$w_m = \frac{1}{E_s}\left[\sigma_s - 0.6\, f_{ctm}\left(\alpha + \frac{1}{\rho_{s,eff}}\right)\right] s_{rm} \geq 0.6 \frac{\sigma_s}{E_s} s_{rm} \tag{7}$$

where f_{ctm} denotes the mean tensile concrete strength. s_{rm} is the average crack distance, i.e. 107.8 mm in the present work (see Table 1). $\rho_{s,eff}$ is the effective tensile steel ratio, which is defined as follows

$$\rho_{s,eff} = \frac{A_s}{b\, h_{c,eff}} \tag{8}$$

where $h_{c,eff} = Min\,(2.5(h - d); (h - X)/3; h/2)$.

In the case of pure bending (i.e. $N = 0$), equation (1) reduces to $S = 0$, and X is written as:

$$X = \frac{\alpha\left(A_s + A_s'\right)}{b}\left[-1 + \sqrt{1 + \frac{2b\left(dA_s + d'A_s'\right)}{\alpha\left(A_s + A_s'\right)^2}}\right] \tag{9}$$

In this case, the curvature and the corresponding tensile steel stress can be calculated substituting $M = Pa/2$ for Ne in equations (4) and (5). The above equations will be used in the next section devoted to the analysis of the curvature and the cracking process in the tested beam.

Curvature Analysis

Following the remark in Section "Curvature Measurement," the existence of an initial longitudinal compressive force in the beam is considered for the analysis of the curvature. It is noticed that equations (1)–(3) depend on the value of X. Therefore, the following procedure is used for the analysis. The longitudinal force N is given an arbitrary constant value. Starting from the value given by equation (9), X is progressively increased, and the corresponding values of S and I

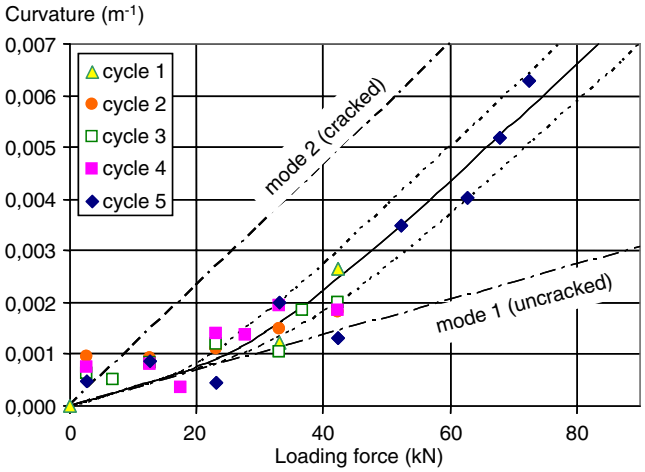

Fig. 12 Experimental curvature from DIC technique (*marks*) and theoretical curvature based on bending plus longitudinal force (*solid* and *dotted lines*) versus loading force—cycles 1–5

are calculated using equations (2) and (3). Finally, the values of χ and P corresponding to the given values of N and X are calculated using equations (4) and (6), respectively.

The experimental values of the curvature derived from the DIC method are compared with the values obtained by this procedure in terms of the loading force in Fig. 12. The two interrupted lines represent the theoretical relationship in pure bending (i.e. without longitudinal force) in mode 1 (uncracked state) and mode 2 (cracked state) respectively. The solid line and the two dotted lines represent the theoretical values obtained for a pre-existing compressive stress equal to 4.2 MPa $\pm$ 1.2 MPa. Despite a discrepancy observed in the experimental results, it is observed that the most of experimental values are located between the two dotted lines for $P > 30$ kN. The difference observed for lower values of P is due to the residual curvature caused by the incomplete closure of the cracks at unloading (see Section "Curvature Measurement"). Therefore, it is possible to conclude that the flexural behaviour of the tested beam is significantly affected by the existence of an initial longitudinal force in the beam. This force could be resulting from a swelling of the concrete due to long term exposition to water steam saturated atmosphere over 25 years of service of the structure.

Crack Width Analysis

The experimental values obtained for the mean crack width are compared to the theoretical values w_m given by equation (7). Firstly, σ_s used in equation (7) is calculated under the assumption of pure bending, i.e. for X given by equation (9) and with substituting $M = Pa/2$ for Ne in equation (5), as it was explained above. The results are shown in Fig. 13 where the theoretical (interrupted line) and the experimental (solid marked lines) values of w_m are plotted against the loading force P. It is obvious that the observed crack opening rate is much lower than expected in pure bending. As for the curvature, this phenomenon can be possibly due to the existence of a longitudinal compressive force in the beam, which causes the cracks to open with a delay.

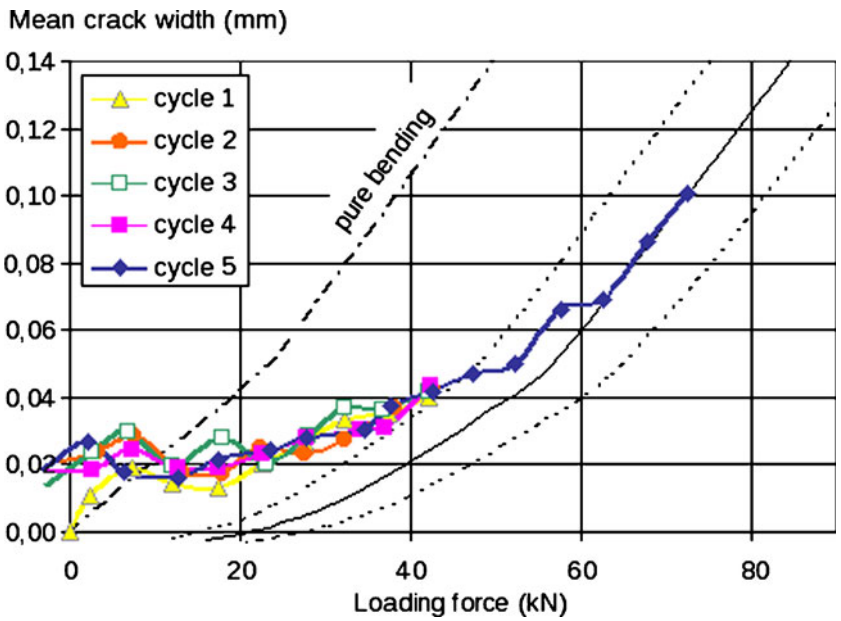

Fig. 13 Mean crack width versus loading force: measured with DIC technique (*marked lines*), and estimated from equation (7) (*solid* and *dotted lines*)—cycles 1–5

In a second stage, the process of crack opening is analyzed under the assumption that a constant longitudinal force exists in the beam. Similarly to the procedure used for the curvature analysis, the longitudinal force N is given a fixed value. X is progressively increased starting from the value given by equation (9), and the values of S, I and e are calculated using equations (2), (3) and (1). Then, the values of χ, P and σ_s are calculated using equations (4), (6) and (5), respectively. Finally, the corresponding values of w_m are calculated using equation (7).

The theoretical values obtained with this procedure are plotted in Fig. 13 against the loading force P. The solid line and the two dotted lines represent the theoretical values obtained for the same pre-existing compressive stress as for the curvature analysis, i.e. 4.2 MPa $\pm$ 1.2 MPa. Although the fit between the theoretical and the experimental curves is not as good as in Fig. 12, the similarity between the theoretical and the experimental curves seems to confirm the influence of a longitudinal force on the process of crack opening during the five loading cycles. Furthermore, the consistency of this conclusion is backed by the perfect correspondence of the pre-existing compressive stress value considered for the curvature analysis and for the crack analysis. It is finally concluded that the flexural behaviour and the cracking process in the tested beam is affected in a similar manner during the five loading cycles by the existence of an initial longitudinal force in the beam.

Conclusion

The actual mechanical behaviour of a full scale reinforced concrete beam was investigated using a digital image correlation technique. Detailed information about the cracking process and the flexural behaviour were easily derived from the analysis of displacement fields processed from digital images of the beam captured at different loading levels. A satisfying resolution about 0.01 mm was achieved for low preparation efforts despite a high length to pixel ratio (0.725 mm/pixel). Main conclusions concerning the measurements and the analysis are listed below.

The DIC technique used in the study proved suitable for early crack detection and measurements. Concrete cracks were located and their widths were precisely measured during five loading cycles in the tensile zone of the beam. A good reproducibility is observed for the mean crack width evolution during the five loading cycles, although large discrepancies are observed between individual crack behaviours. One of advantages of the method is that cracks can be detected and their widths measured as soon as they appear. Details such as residual crack widths due to interlocking effect at unloading are observed.

Precise information concerning the deflection and the curvature of the bent beam were derived from the displacement fields given by the DIC technique. Values of the mid-span deflection obtained with the DIC technique are in fair agreement with values measured by the LVDT sensor. A bimodal behaviour is evidenced, which suggests the existence of a compressive stress state in the beam cross-section. This hypothesis is supported by the existence of a delay observed in the evolution of crack openings during application of the loading force. A theoretical analysis based on Eurocode 2 design code provisions in the serviceability state leads to the conclusion that the cracking and the flexural behaviour of the tested beam are significantly affected by the existence of initial compressive stresses in the beam cross-section. This initial stress state could possibly result from swelling of the concrete during the 25 years of service in wet atmosphere and elevated temperature.

Finally, this work hightlights that DIC technique is suitable for the analysis of deformation and cracking process in full scale reinforced concrete members. One of main advantages is that it allows easy crack detection and measurements for limited preparation works. The research and the experimental program done in this study open the possibility of applying DIC technique for detailed damage assessment of existing civil structures. Although the present study was carried out in laboratory, one could as well imagine to conduct such a study *in situ* in a near future.

References

1. Sutton MA, Wolters WJ, Perters WH, Ranson WF, McNeill SR (1983) Determination of displacements using an improved digital correlation method. Image Vis Comput 1(3):133–139
2. Sutton MA (2008) Digital image correlation for shape and deformation measurements. In: Springer handbook of experimental solid mechanics, vol 208(C), pp 565–600
3. Périé J-N, Calloch S, Cluzel C, Hild F (2002) Analysis of a multiaxial test on a C/C composite by using digital image correlation and a damage model. Exp Mech 42(3):318–332
4. Robert L, Nazaret F, Cutard T, Orteu J-J (2007) Use of 3-D digital image correlation to characterize the mechanical behavior of a fiber reinforced refractory castable. Exp Mech 47:761–773
5. Muller M, Toussaint E, Destrebecq J-F, Grédiac M (2004) Experimental and numerical study of reinforced concrete specimens strengthened with composite plates. Compos, Part A 35:885–893

6. Choi S, Shah SP (1997) Measurement of deformations on concrete subjected to compression using digital image correlation. Exp Mechs 37(3):307–313
7. Tung S-H, Shih M-H, Sung W-P (2008) Development of digital image correlation technique to analyse crack variations on masonry wall. Sadhana 33(6):767–779
8. Lecompte D, Vantomme J, Sol H (2006) Crack detection in a concrete beam using two different camera techniques. Structural Health Monitoring 5(59):59–68
9. Helm JD (2008) Digital image correlation for specimens with multiple growing cracks. Exp Mech 48:753–762
10. Avril S, Hamelin P, Vautrin A, Surrel Y, Sutton MA (2005) A multi-scale approach for crack width prediction in reinforced-concrete beams repaired with composites. Compos Sci Technol 65(3–4):445–453
11. Küntz M, Jolin M, Bastien J, Perez F, Hild F (2006) Digital image correlation analysis of crack behavior in a reinforced concrete beam during a load test. Can J Civ Eng 33:1418–1425
12. CEN (2003) Eurocode 2. Design of concrete structures. Part 1: general rules and rules for buildings. EN 1992-1:2003. European Committee for Standardization (CEN), Brussels
13. Vacher P, Dumoulin S, Morestin F, MGuil-Touchal S (1999) Bidimensional strain measurement using digital images. Proc Inst Mech Eng 213(C):811–817
14. Hild F, Roux S, Gras R, Guerrero N, Marante EM, Florez-Lopez J (2009) Displacement measurement technique for beam kinematics Opt Lasers Eng 47:495–503
15. Rethore J, Hild F, Roux S (2008) Extended digital image correlation with crack shape optimization Int J Numer Methods Eng 73:248–272